Department of Mathematics and Statistics
College of Engineering

UC
UNIVERSITY OF CANTERBURY
Te Whare Wānanga o Waitaha
CHRISTCHURCH NEW ZEALAND

Summer Research Project

Chaos from Simplicity:

An Introduction to the Double Pendulum

by Joe Chen

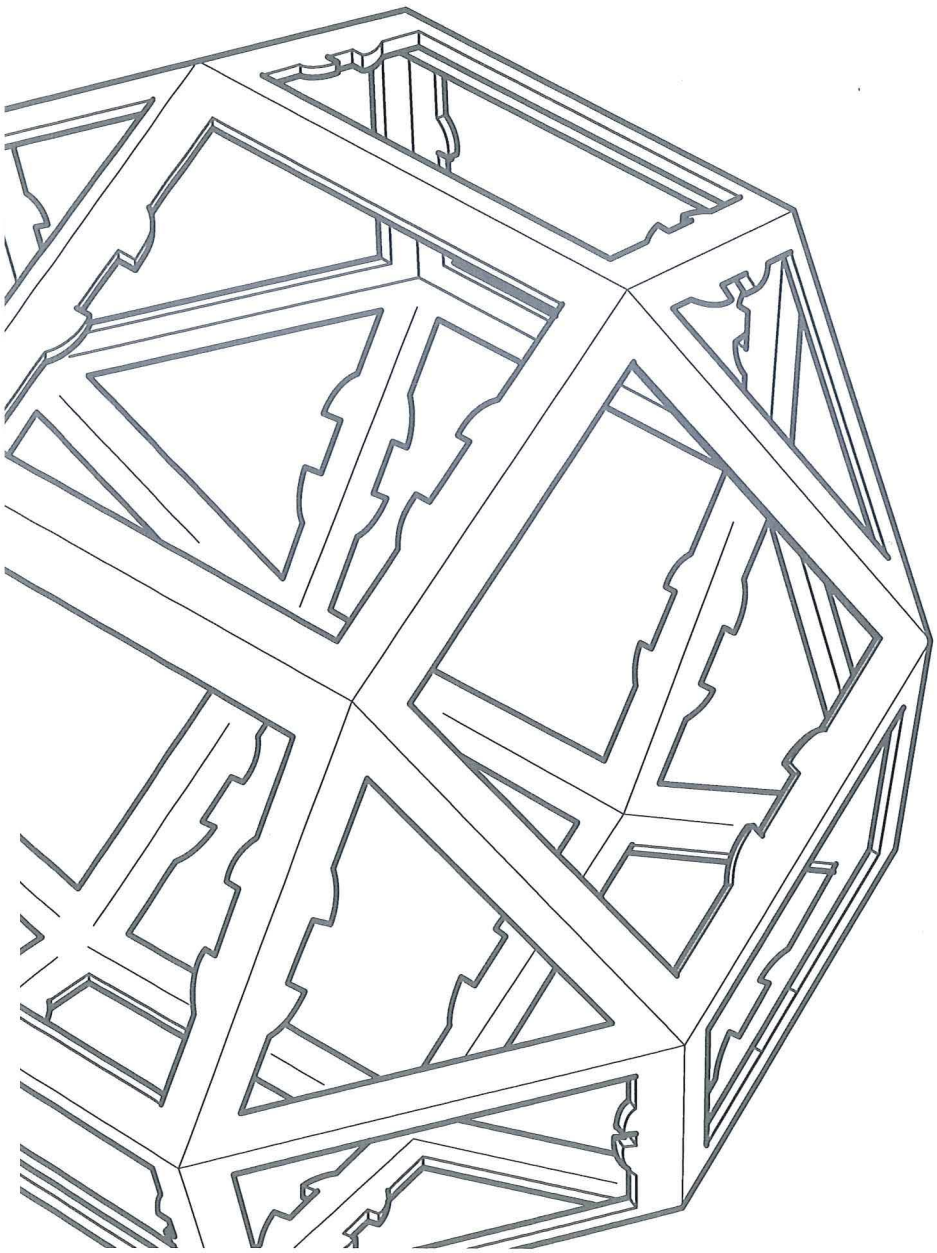

08

Chaos from Simplicity: An Introduction to the Double Pendulum

Joe Chen

5 February 2008

Abstract

The fusion of two pendulums give rise to a simple mechanical system that on contrary to its deceptively simple appearances exhibit extremely unpredictable and complex behaviour. The equations of motion for the simple double pendulum are derived, and they are used to generate phase portraits and plots of time-for-first-flip. Lyapunov exponents are also computed and show that the larger the release angle of the pendulum, the more sensitive to initial conditions the system becomes. Damping and forcing are then introduced and a brief investigation into the strange attractor of the double pendulum illustrates its chaotic nature.

1 Introduction

The double pendulum consists of two pendulums attached together with the pivot of the second pendulum located at the end of the first. This means one pendulum is suspended freely from another but are both constrained to oscillate in the same plane.

The coupled influence of the two pendulum masses on each other cause complex behaviours first formally studied by Euler and Daniel Bernoulli in 1738. They considered different modes of oscillations and even generalised to n-multiple pendulum systems [2]. Euler and Bernoulli were working on these problems in the period of time when it had become clear that differential equations of motion would be the key to virtually all dynamical problems [13]. However it wasn't until the advent of powerful processors and efficient computers that systems such as the double pendulum can be studied in more detail since the solutions to its governing equations in most cases can only be solved numerically. The discovery of rich and complicated dynamics once these equations are solved shows the chaotic nature of the double pendulum; where its apparently deterministic motion are actually unpredictable.

Investigations into the double pendulum system may not only yield theoretical treasures but also provide practical applications as well. For example, test masses already suspended at LIGO (Laser Interferometer Gravitational Wave Observatory) comprises of a double pendulum system [4]; its purpose is to help filter seismic noise from the gravitational waves awaiting detection.

Another physical application of the double pendulum is utilising its somewhat close resemblance to human arms joined together at certain degrees and can thus be used to model the swinging motion of athletes for finding optimal performances in sports such as golf [14]; see figure 1.

In this paper we will concentrate only on simple double pendulum systems, where the system consists of point masses connected by rigid, massless rods; as shown in figure 3. This is because the more realistic considerations of physical double pendulums (figure 2) behave similarly but needs an extra rotational inertia term which only complicates matter unnecessarily.

We begin by deriving the system of differential equations governing the motion of the double pendulum, then plot some of its trajectories by numerically solving these equations in MATLAB. From there, some investigations are carried out to demonstrate the chaotic behaviour of the double pendulum - looking at the

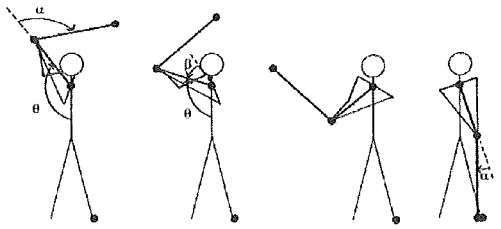

Figure 1: Modelling the golf swing with double pendulums; adapted from [14].

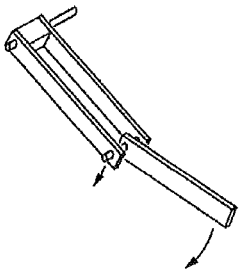

Figure 2: Physical double pendulum; adapted from paper by Shinbrot et al. [15].

time required for the pendulums to flip, and calculating the Lyapunov exponents to give a measure of the sensitivity to changes in initial conditions. Damping and forcing will then be introduced into the system and then we briefly investigate the strange attractors of the double pendulum.

2 Derivation of the Equations of Motion

The motion of the double pendulum can be described by two coupled ordinary second order differential equations. We will derive them here using the standard method of Lagrangian mechanics; full details can be found in [1]. Originally formulated by Lagrange in 1788, this method use energy considerations rather than forces to derive the equations of motion [8].

First define the positions and the velocities of the pendulum masses using the angles they make with the vertical; θ_1 and θ_2.

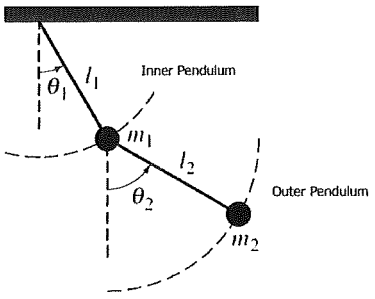

Figure 3: Labelled simple double pendulum.

Positions

$$
\begin{aligned}
x_1 &= l_1 \sin\theta_1 \\
y_1 &= -l_1 \cos\theta_1 \\
x_2 &= x_1 + l_2 \sin\theta_2 = l_1 \sin\theta_1 + l_2 \sin\theta_2 \\
y_2 &= y_1 - l_2 \cos\theta_2 = -l_1 \cos\theta_1 - l_2 \cos\theta_2
\end{aligned}
$$

Velocities

$$
\begin{aligned}
\dot{x}_1 &= l_1\dot{\theta}_1 \cos\theta_1 \\
\dot{y}_1 &= l_1\dot{\theta}_1 \sin\theta_1 \\
\dot{x}_2 &= \dot{x}_1 + l_2\dot{\theta}_2 \cos\theta_2 = l_1\dot{\theta}_1 \cos\theta_1 + l_2\dot{\theta}_2 \cos\theta_2 \\
\dot{y}_2 &= \dot{y}_1 + l_2\dot{\theta}_2 \sin\theta_2 = l_1\dot{\theta}_1 \sin\theta_1 + l_2\dot{\theta}_2 \sin\theta_2
\end{aligned}
$$

The total kinetic energy T of the double pendulum system can be expressed as the sum of the kinetic energies of each individual components x_1, y_1, x_2, y_2, so

$$T = \frac{1}{2}m_1(\dot{x}_1^2 + \dot{y}_1^2) + \frac{1}{2}m_2(\dot{x}_2^2 + \dot{y}_2^2).$$

Substituting in the velocities defined previously and then simplifying, the kinetic energy of the double pendulum system can be expressed in terms of θ_1 and θ_2, giving

$$T = \frac{1}{2}(m_1 + m_2)l_1^2\dot{\theta}_1^2 + \frac{1}{2}m_2 l_2^2\dot{\theta}_2^2 + m_2 l_1 l_2 \dot{\theta}_1\dot{\theta}_2 \cos(\theta_1 - \theta_2). \tag{1}$$

The potential energy $U = mgh$ can be expressed similarly where h is the net vertical height above the zero-energy point when the pendulum is in its equilibrium position $\theta_1 = \theta_2 = 0$, so

$$U = m_1 g y_1 + m_2 g y_2.$$

Substituting for y_1 and y_2 and simplifying as before, the potential energy of the double pendulum system is

$$U = -g\big((m_1 + m_2)l_1 \cos\theta_1 + m_2 l_2 \cos\theta_2\big). \tag{2}$$

So the Lagrangian $L = T - U$ becomes

$$L = \frac{1}{2}(m_1 + m_2)l_1^2\dot{\theta}_1^2 + \frac{1}{2}m_2 l_2^2\dot{\theta}_2^2 + m_2 l_1 l_2 \dot{\theta}_1\dot{\theta}_2 \cos(\theta_1 - \theta_2) + g(m_1 + m_2)l_1 \cos\theta_1 + g m_2 l_2 \cos\theta_2. \tag{3}$$

Now we can apply a result from calculus of variations known as the Euler-Lagrange equation [13]. This relation will enable us to derive the equations of motion by simply using the Lagrangian in equation (3). The Euler-Lagrange equation in terms of generalised coordinates can be expressed as:

$$\frac{d}{dt}\left(\frac{\partial L}{\partial \dot{q}_i}\right) - \frac{\partial L}{\partial q_i} = 0, \tag{4}$$

where $i = 1, \ldots, n$ and q_i represent the ith general coordinate [17]. Altogether the number of general coordinates n equals the number of degrees of freedom of the system. In the case of the double pendulum there are two degrees of freedom so $q_1 = \theta_1$ and $q_2 = \theta_2$.

For θ_1 the Euler-Lagrange equation becomes

$$\frac{d}{dt}\left(\frac{\partial L}{\partial \dot{\theta}_1}\right) - \frac{\partial L}{\partial \theta_1} = 0. \tag{5}$$

We can determine each parts separately, giving

$$\frac{\partial L}{\partial \theta_1} = -m_2 l_1 l_2 \dot{\theta}_1 \dot{\theta}_2 \sin(\theta_1 - \theta_2) - l_1 g (m_1 + m_2) \sin\theta_1,$$

and

$$\begin{aligned}\frac{d}{dt}\left(\frac{\partial L}{\partial \dot{\theta}_1}\right) &= \frac{d}{dt}\left((m_1 + m_2) l_1^2 \dot{\theta}_1 + m_2 l_1 l_2 \dot{\theta}_2 \cos(\theta_1 - \theta_2)\right) \\ &= (m_1 + m_2) l_1^2 \ddot{\theta}_1 + m_2 l_1 l_2 \left(\ddot{\theta}_2 \cos(\theta_1 - \theta_2) - \dot{\theta}_2 (\dot{\theta}_1 - \dot{\theta}_2) \sin(\theta_1 - \theta_2)\right).\end{aligned}$$

Now expand and substitute these parts back into equation (5); finally, cancel out terms and divide through by l_1 to give us one of the two equations of motion for the double pendulum; shown in equation (6). Similarly, by performing the same procedure using the Euler-Lagrange equation for θ_2,

$$\frac{d}{dt}\left(\frac{\partial L}{\partial \dot{\theta}_2}\right) - \frac{\partial L}{\partial \theta_2} = 0,$$

we can obtain the second equation of motion given in equation (7).

So the pair of coupled second order differential equations governing a simple double pendulum are:

$$(m_1 + m_2) l_1 \ddot{\theta}_1 + m_2 l_2 \ddot{\theta}_2 \cos(\theta_1 - \theta_2) + m_2 l_2 \dot{\theta}_2^2 \sin(\theta_1 - \theta_2) + (m_1 + m_2) g \sin\theta_1 = 0 \tag{6}$$

$$m_2 l_2 \ddot{\theta}_2 + m_2 l_1 \ddot{\theta}_1 \cos(\theta_1 - \theta_2) - m_2 l_1 \dot{\theta}_1^2 \sin(\theta_1 - \theta_2) + m_2 g \sin\theta_2 = 0 \tag{7}$$

These highly non-linear differential equations give some hints that the behaviour of the double pendulum is going to be quite complicated. Notice that equation (7) is actually independent of masses; since m_2 can be cancelled out, but it is left in for symmetry.

In order to solve these equations numerically, we need to turn these two coupled second order equations into a system of four first order equations. Upon rearranging and setting the time derivative of the angles $\dot{\theta}_1$ and $\dot{\theta}_2$ to equal the angular velocities ω_1 and ω_2 respectively, and letting $\theta_1 - \theta_2 = \Delta\theta$, we get the system

$$\begin{aligned}\omega_1 &= \dot{\theta}_1, \\ \omega_2 &= \dot{\theta}_2, \\ \dot{\omega}_1 &= \frac{m_2 l_1 \omega_1^2 \sin(2\Delta\theta) + 2 m_2 l_2 \omega_2^2 \sin\Delta\theta + 2 g m_2 \cos\theta_2 \sin\Delta\theta + 2 g m_1 \sin\theta_1}{-2 l_1 (m_1 + m_2 \sin^2\Delta\theta)}, \\ \dot{\omega}_2 &= \frac{m_2 l_2 \omega_2^2 \sin(2\Delta\theta) + 2(m_1 + m_2) l_1 \omega_1^2 \sin\Delta\theta + 2 g (m_1 + m_2) \cos\theta_1 \sin\Delta\theta}{2 l_2 (m_1 + m_2 \sin^2\Delta\theta)}.\end{aligned} \tag{8}$$

This is the set of equations needed to plug into the numerical differential equation solver in MATLAB.

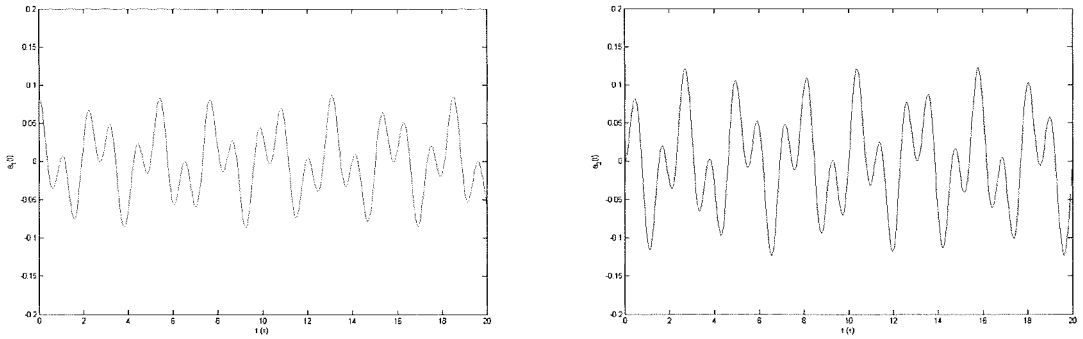

(a) (b)

Figure 4: Motion for small-angle-release with initial conditions $\theta_1(0) = 5^o$ and $\theta_2(0) = 0^o$. (a) shows the behaviour of the time series for θ_1 and (b) the behaviour for θ_2.

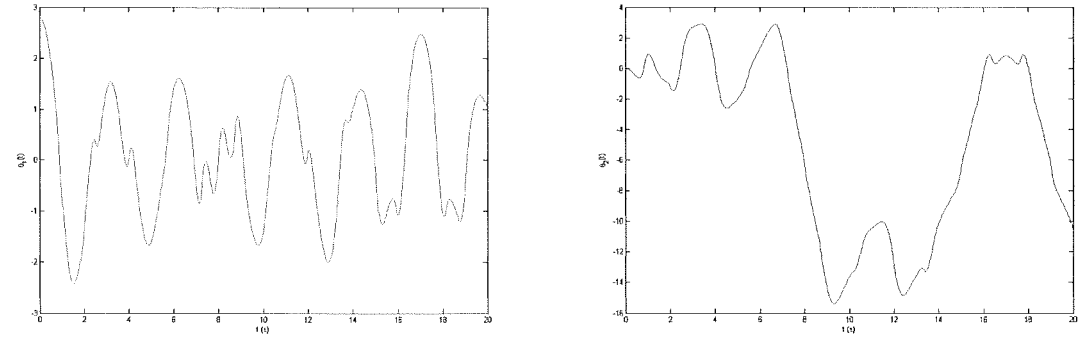

(a) (b)

Figure 5: Motion for large-angle-release with initial conditions $\theta_1(0) = 160^o$ and $\theta_2(0) = 0^o$. (a) shows the behaviour of the time series for θ_1 and (b) the behaviour for θ_2.

3 Trajectories of the Double Pendulum

Now that the two coupled second order differential equations of motion are expressed as a system of four first order equations, they can be readily solved numerically to give the trajectories of the double pendulum at specified initial conditions. The parameters of the double pendulum used in the investigations of this paper are defined to be equal mass pendulum bobs and equal length connecting rods with all of them normalised to be 1 units, in other words the parameters are

$$\begin{aligned} m_1 = m_2 &= 1\text{kg}, \\ l_1 = l_2 &= 1\text{m}, \end{aligned} \tag{9}$$

and we refer to these values as the "unity parameters".

The system is solved using the MATLAB command: ode113. Originally, the command ode45 was used, but many problems were encountered when it was applied on the equations. One such difficulty was that the speed of ode45 was considerably slower than ode113, sometimes taking up to 3 minutes whereas ode113 is

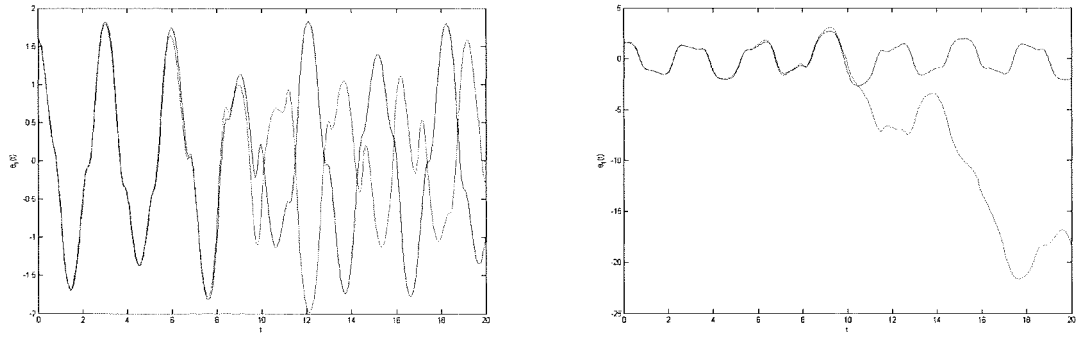

(a) (b)

Figure 6: Sensitivity to changes in initial condition. Blue path has $\theta_1(0) = \theta_2(0) = 90°$. Red path has $\theta_1(0) = \theta_2(0) = 91°$ resulting in a 1° difference in the initial release. (a) compares the behaviour for θ_1 and (b) the behaviour for θ_2. Entirely different trajectories resulted after only 10 seconds.

finished in 30 seconds and still give the same result. Another more significant problem is encountered later and is described in the next section. Overall, ode113 gave a much better result and was therefore adopted as the command for solving the equations of motion of the double pendulum for the rest of the investigation.

When the system of equations are solved and plotted, they give a picture showing how the angles θ_1 and θ_2 to the vertical of the inner and outer pendulum masses respectively change with time. Some representative trajectories of the double pendulum are displayed; figure 4 shows the motion of a 5° small-angle-release. We can see that for the initial release angles being small, the double pendulum behaves like a linear oscillator with relatively regular oscillations having almost constant amplitude and period. Large-angle-release is shown in figure 5 where the release angle is 160°. The wild and erratic behaviour corresponds well to the actual motion of the double pendulum.

Notice that the scale for the small angle motion ranges only from -0.2 to 0.2 radians whereas the motion for θ_2 in the large-angle-release at one time plunges from around 3 to -15 radians indicating that the outer pendulum mass performed almost six consecutive revolutions. This illustrates the vast scope of behaviour the double pendulum can exhibit given the right initial conditions.

If we plot two trajectories that have very close initial conditions together; as in figure 6 with the blue and red trajectory differ by only 1° upon release, something interesting is observed. The paths initially stay fairly close together and then suddenly diverges considerably. Figure 6(a) shows that after only about 10 seconds, the paths become very much distinct; being completely out of phase with each other. This phenomenon of growth of small differences in the starting state is called the sensitive dependence on initial conditions [5].

For another demonstration of the sensitivity to initial conditions of the double pendulum system, it is interesting to note that when the motion equations of the system is changed to a different form with for example $\sin(2\Delta\theta)$ replaced by $2\sin\Delta\theta\cos\Delta\theta$ in equation (8), different trajectories were obtained when the equations are solved; as shown in figure 7 - even though we know that the equations are still actually the same since

$$\sin(2\Delta\theta) \equiv 2\sin\Delta\theta\cos\Delta\theta.$$

This apparent paradox is due to the errors introduced by finite computing processes. Different forms of the same equation means different ways of calculating the same thing, which will lead to the accumulation of different errors over the many steps required to solve the equations. The double pendulum's sensitivity to

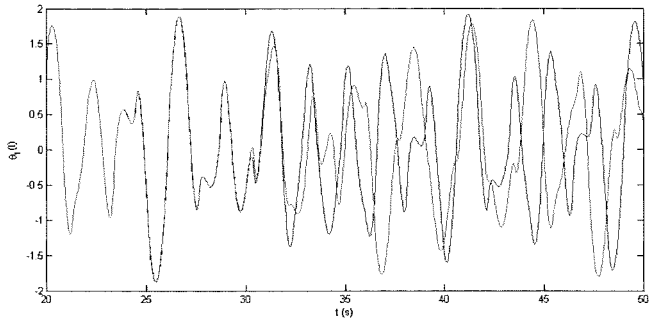

Figure 7: Another demonstration of the sensitivity to initial conditions of the double pendulum where part of the equation of motion is altered; $\sin(2\Delta\theta)$ (blue) changed to $2\sin\Delta\theta\cos\Delta\theta$ (red). Trajectories become distinct after only 30 seconds from release; theoretically they should remain the same for all values of time t but in practice, errors will be introduced in the computation.

change then comes into play and make these errors increase exponentially, thus vastly different trajectories resulted over time. These extreme sensitivity to changes in initial conditions is a hallmark of chaos [9] and is treated in more detail later.

4 Time for First Flip

For one of the pendulum masses in the double pendulum system to "flip" means the mass has gone over the top of its path where it has essentially rotated to its inverted position $\theta = \pi$. The time-for-first-flip (TFF) of a pendulum is the time it takes for that pendulum mass to flip for the first time since it was released at $t = 0$. The pendulum mass need not continue through to perform a full rotation by 360°, in fact it could even go past its inverted position then suddenly flip back and it would still satisfy the criteria for TFF. We are only interested in the time it takes to reach the inverted position for the first time.

As mentioned in the last section, attempting to use the MATLAB command ode45 to solve the system of double pendulum equations of motion met with many difficulties. One of the major problems is that the total energy of the system did not remain constant at an acceptable level. Since we are considering a hypothetical double pendulum system where friction, air resistance, noise, and other dissipative forces are ignored, we expect energy to be conserved; i.e. the total energy of the system should remain constant. Even though the finite computational power of any numerical methods will inevitably introduce some degree of errors; those that were associated with ode45 was much too great to ignore; see figure 8. The total energy of the system increases steadily when ode45 was used, which means pendulum flip would occur when it should not have.

4.1 Theoretical Boundaries of Pendulum Flip

Using energy considerations, the minimum condition required for pendulum 1, the inner pendulum, to flip is when $\theta_1 = \pi$ and $\theta_2 = 0$. Similarly for pendulum 2, the outer pendulum, the minimum condition is when $\theta_1 = 0$ and $\theta_2 = \pi$. Now using the general potential energy expression defined earlier by equation (2), plug in the minimum condition to flip for pendulum 1 and we get the least energy, U_{min1}, required for the inner pendulum to flip,

$$U_{min1} = g\big(l_1(m_1 + m_2) - l_2 m_2\big). \tag{10}$$

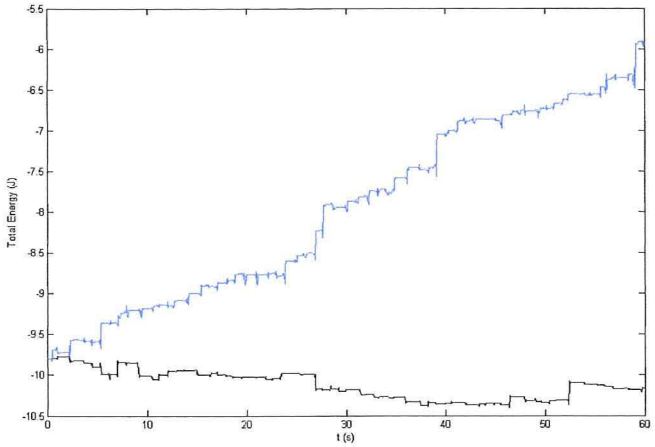

Figure 8: Comparison of the total energy of the double pendulum system solved numerically using ode45 (blue) and ode113 (black). The progressive increase in the total energy of the system using ode45 will give erroneous results of pendulum flip. Notice ode113 results in far more constant total energy.

For the respective pendulum masses to flip, its potential energy U must be greater than or equal to its U_{min}, so for pendulum 1,

$$U \geq U_{min1}.$$

Substituting for their respective general expressions from equation (2) and equation (10), then rearrange to get

$$l_1(m_1 + m_2)(\cos\theta_1 + 1) + l_2 m_2(\cos\theta_2 - 1) \leq 0,$$

and similarly for pendulum 2,

$$l_1(m_1 + m_2)(\cos\theta_1 - 1) + l_2 m_2(\cos\theta_2 + 1) \leq 0.$$

Finally, applying the unity parameters in equation (9), we get the constraint equations respectively for pendulum 1 and pendulum 2 to flip:

$$2\cos\theta_1 + \cos\theta_2 \leq -1, \tag{11}$$
$$2\cos\theta_1 + \cos\theta_2 \leq 1. \tag{12}$$

So for initial release angles θ_1 and θ_2 not satisfying these constraints will result in the respective pendulum masses not having enough energy to flip. Figure 9 shows the geometric shape of these constraints.

4.2 TFF Plots

The time for first flip essentially tells us something about the energy of the double pendulum in relation to the starting position of the system. When TFF is measured against different initial conditions, it can be used to gain insight into the chaotic nature of the double pendulum.

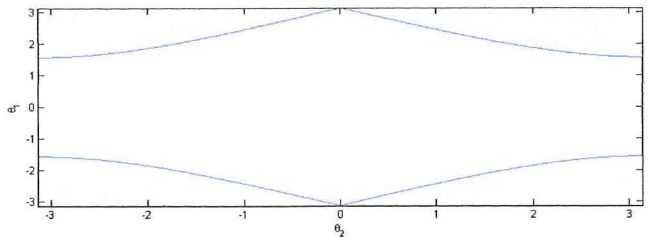

(a)

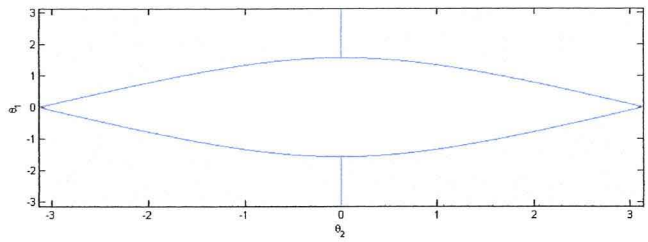

(b)

Figure 9: Boundaries for the criteria to flip. (a) shows boundary for the inner pendulum mass given in equation (11), and (b) shows boundary for the outer pendulum mass given in equation (12). Shaded regions indicate where the pendulum mass has enough energy to flip.

After large amounts of CPU run-time, initial starting positions of the inner and outer pendulums are systematically looped through to find the time-for-first-flip for each initial conditions. Starting at 0 radians, initial conditions are iterated through to π radians with increments of $\frac{\pi}{200}$. This is done for the two pendulum masses with respect to each other, so there are a total of $200 \times 200 = 40000$ individual trajectories evaluated. A 3-dimensional plot can now be obtained by plotting starting points $\theta_1(0)$ and $\theta_2(0)$ on the x and y axis, and TFF value corresponding to those initial conditions on the z axis.

Because the left and right side of the double pendulum are symmetrical, the plot generated has rotational symmetry and can be rotated by 180° about the origin to obtain the complete picture for the TFF of all the initial conditions. Figures 10(a) and 10(b) show the contour plots of these 3D surfaces. The interesting patterns and rich dynamics of these figures demonstrate the complexity of the double pendulum.

In these figures, the double pendulum equations were evaluated to 70 seconds, so TFF up to 70 seconds are detected. The white parts of the plot indicate the pendulum mass has not flipped during this time. Notice that the curvature of the main white region of the pattern where the pendulum masses never has enough energy to flip, corresponds exactly with the constraint equations derived earlier. This can be seen clearly by comparing the TFF plots with the boundary of the constraints shown in figure 9(a) and 9(b).

As mentioned earlier, the double pendulum has a vertical line of symmetry right down its middle, so this indicates that the phase space of the double pendulum system has cylindrical properties just like a normal singular pendulum [10], which means the plots can be joined together by curving the edges so that one side matches the other. Now, if we zoom in on the TFF contour plots, we can see similar shapes and swirling patterns continuing to persist. When this pattern of points has similar details on finer and finer scales, the term *fractal* is often applied [12] and this is the case for the time-for-first-flip contour plot. This self-similarity is displayed by figure 11 showing the enlarged view of a small part of the top right quadrant in figure 10(b) where a white section extends into the region that could exhibit pendulum flip.

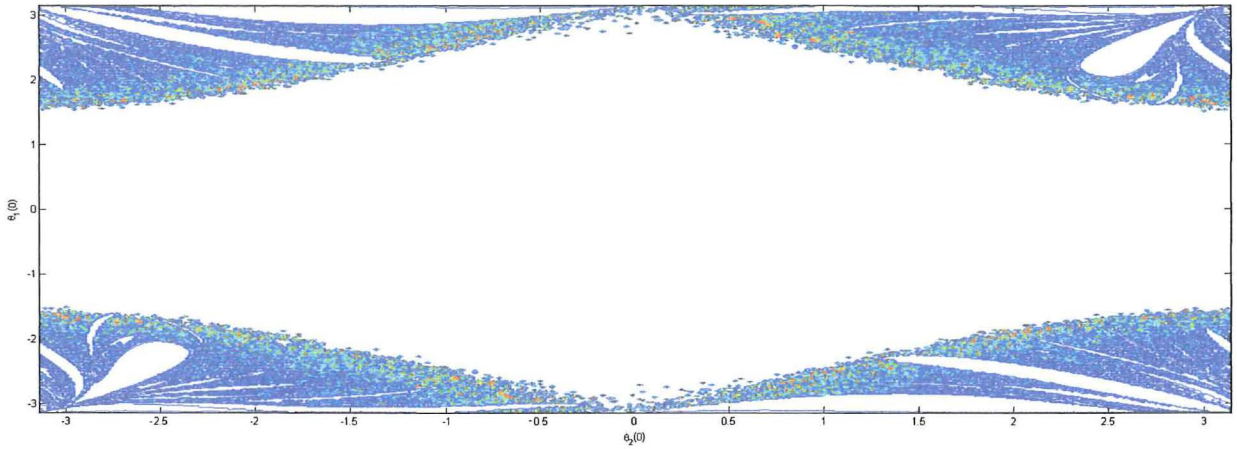

(a)

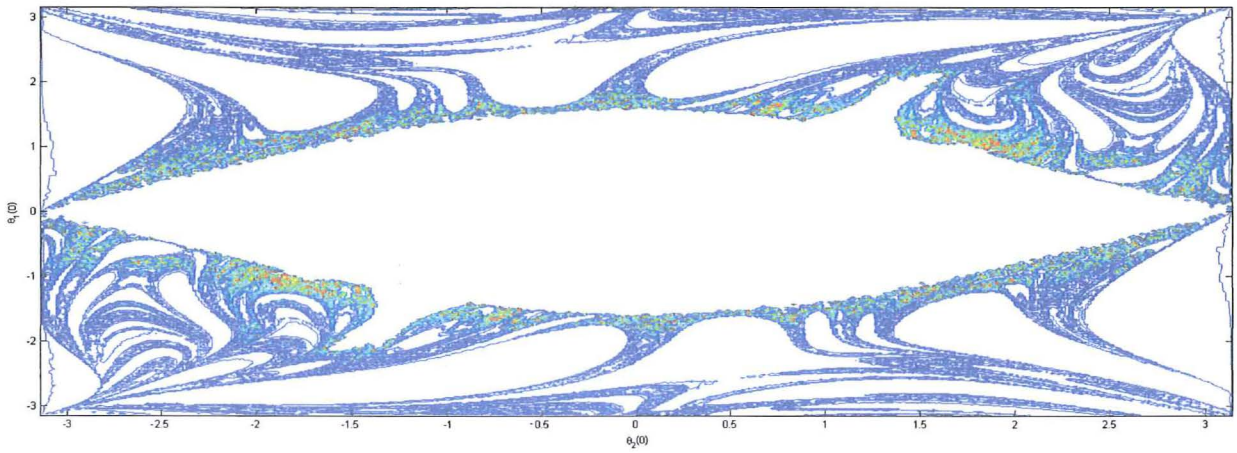

(b)

Figure 10: Contour plots for the time-for-first-flip of the respective pendulum masses; (a) giving the plot for the inner pendulum, (b) the outer pendulum. Axis shows initial conditions $\theta_1(0)$ along the y-direction and $\theta_2(0)$ along the x-direction. Blue region needs less time to flip, red region needs more time, white regions do not flip at all in the 70 seconds evaluated. Curious patterns emerge which has rotational symmetry.

5 Damped and Forced Double Pendulum

Now we consider double pendulum systems that take into account damping effects and external forces. The damping force on the pendulum masses μ, is approximated to be proportional to the angular velocity of the respective pendulum mass, giving

$$\mu = k\dot{\theta},$$

where k is a constant describing the damping.
Next, the periodic external force F applied at a frequency φ on the pendulum masses can be described by

$$F(t) = F\cos\varphi t,$$

and this force is applied in a direction tangent to the motion of the pendulum masses.

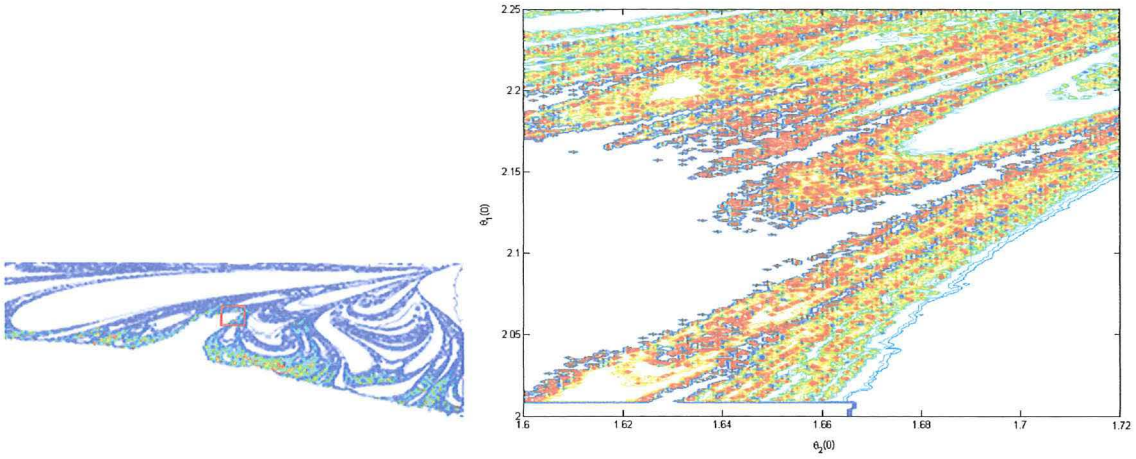

Figure 11: Zoomed in view of part of the TFF contour plot in figure 10(b) showing self-similar patterns and possible fractal structures.

Using these definitions and the subscripts 1 and 2 to denote the respective damping constant and forcing amplitude on the inner and outer pendulums, the equations of motion for the damped and forced double pendulum system are therefore:

$$(m_1+m_2)l_1\ddot{\theta}_1 + m_2l_2\ddot{\theta}_2\cos(\theta_1-\theta_2) + m_2l_2\dot{\theta}_2^2\sin(\theta_1-\theta_2) + (m_1+m_2)g\sin\theta_1 + k_1\dot{\theta}_1 = F_1\cos\varphi_1 t$$
$$m_2l_2\ddot{\theta}_2 + m_2l_1\ddot{\theta}_1\cos(\theta_1-\theta_2) - m_2l_1\dot{\theta}_1^2\sin(\theta_1-\theta_2) + m_2g\sin\theta_2 + k_2\dot{\theta}_2 = F_2\cos\varphi_2 t.$$

If we let

$$\alpha = k_1\dot{\theta}_1 - F_1\cos\varphi_1 t, \tag{13}$$
$$\beta = k_2\dot{\theta}_2 - F_2\cos\varphi_2 t, \tag{14}$$

and then introduce the angular velocity ω as before, we can find the system of four first order equations after some rearranging, giving

$$\begin{aligned}
\omega_1 &= \dot{\theta}_1,\\
\omega_2 &= \dot{\theta}_2,\\
\dot{\omega}_1 &= \frac{m_2l_1\omega_1^2\sin(2\Delta\theta) + 2m_2l_2\omega_2^2\sin\Delta\theta + 2gm_2\cos\theta_2\sin\Delta\theta + 2gm_1\sin\theta_1 + \gamma_1}{-2l_1(m_1+m_2\sin^2\Delta\theta)},\\
\dot{\omega}_2 &= \frac{m_2l_2\omega_2^2\sin(2\Delta\theta) + 2(m_1+m_2)l_1\omega_1^2\sin\Delta\theta + 2g(m_1+m_2)\cos\theta_1\sin\Delta\theta + \gamma_2}{2l_2(m_1+m_2\sin^2\Delta\theta)},
\end{aligned} \tag{15}$$

where

$$\gamma_1 = 2\alpha - 2\beta\cos\Delta\theta,$$
$$\gamma_2 = 2\alpha\cos\Delta\theta - \frac{2(m_1+m_2)}{m_2}\beta.$$

This is the same system of four equations as before in equation (8) with the extra terms γ_1 and γ_2 added in the numerator. For our definition of damping and forcing, α and β are those in equation (13) and (14).

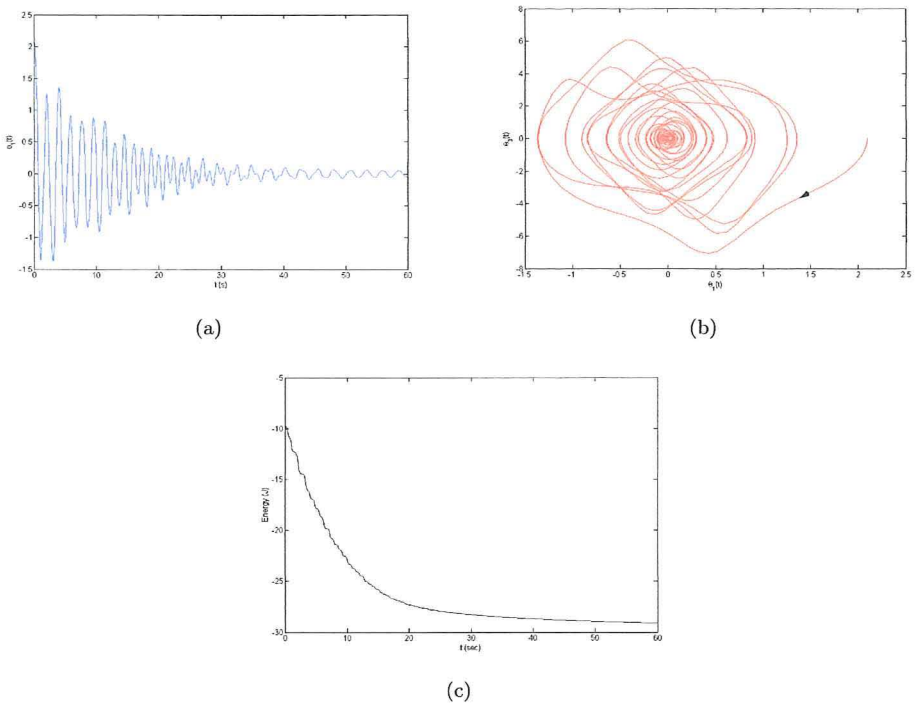

(a) (b)

(c)

Figure 12: Pure damping motion of the double pendulum with no forcing. Damping constant is small: $k_1 = k_2 = 0.1$ and behaviour of the first minute after release is shown. All figures have initial conditions $\theta_1(0) = 120°, \theta_2(0) = 0°$ and no initial angular velocities. (a) shows the time series of θ_1, (b) gives the trajectory of θ_1 vs $\dot{\theta}_1$, with arrows indicating the direction of the path through phase space, and (c) shows the behaviour of the total energy of the system.

Our new system of equations can be solved in the same way as before to obtain the trajectories for double pendulums with damping and forcing.

As expected with pure damping, the double pendulum system loses energy and its motion settles into the stable equilibrium position at $\theta_1 = \theta_2 = 0°$. These behaviours are shown in figure 12 with small damping, and in figure 13 with relatively larger damping. Notice for the large damping the total energy decreases significantly faster, dropping almost to the zero-energy point within 10 seconds.

Adding in damping along with an external periodic force, and trajectories such as those in figure 14 are obtained. After around 20 seconds, the chaotic motion of the double pendulum itself is overridden by the damping effects and only the motion due to the continuous external force remains.

6 Lyapunov Exponent

As mentioned earlier, the double pendulum system is extremely sensitive to changes in initial conditions. Seemingly indistinguishable discrepancies at the start can lead to vastly dissimilar trajectories at the end. More precisely, if we start with two nearby generic initial conditions separated by d_0, the distance after time t between the orbits in phase space, $d(t)$, grows exponentially for short intervals of time on the average. This is one of the critical aspects of chaos [3]. Thus giving

$$d(t) = d_0 e^{\lambda t}, \tag{16}$$

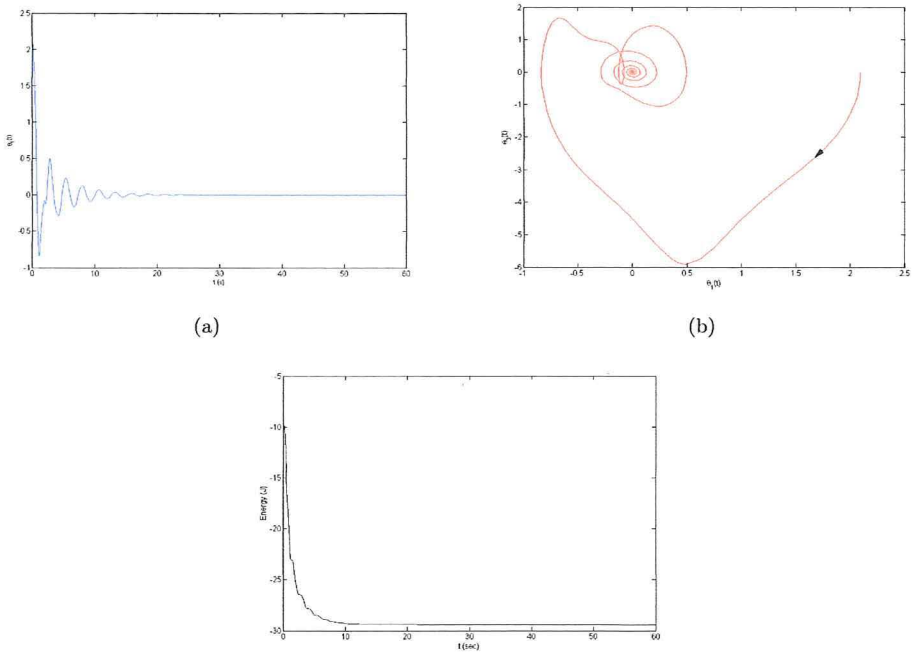

(a) (b)

(c)

Figure 13: As figure 12, pure damping motion with no forcing but now with a larger damping constant: $k_1 = k_2 = 1$. Again, all figures have initial conditions $\theta_1(0) = 120^o, \theta_2(0) = 0^o$ and no initial angular velocities. (a) shows the time series of θ_1, (b) gives the trajectory of θ_1 vs $\dot{\theta}_1$, with arrows indicating the direction of the path through phase space, and (c) shows the behaviour of the total energy of the system.

where λ is the Lyapunov exponent. This gives us a quantitative measurement of the sensitivity.

This exponential growth in separations for the double pendulum is illustrated well by Gleick in his book *Chaos: Making a New Science* [6]

> "the dependence on initial conditions was so sensitive that the gravitational pull of a single raindrop a mile away mixed up the motion within two minutes."

The divergence of the double pendulum trajectories can only be locally exponential since $d(t)$ cannot go to infinity due to the system being physically bounded. So to find the Lyapunov exponent we must average the exponential growth at many points along a trajectory [11]. Using the definition of the Lyapunov exponent in equation (16) we can derive an expression to find the average λ from a total of n intermediate λ_i values evaluated. So starting with

$$d(t_i) = d_0 e^{\lambda_i (t_i - t_{i-1})},$$

where $i = 1, \ldots, n$ and rearrange to get

$$\lambda_i = \frac{1}{t_i - t_{i-1}} \ln\left(\frac{d(t_i)}{d_0}\right)$$

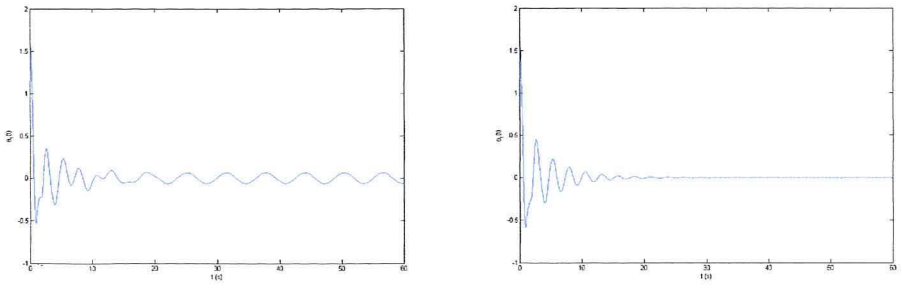

(a) $(1, 1)$ (b) $(1, 10)$

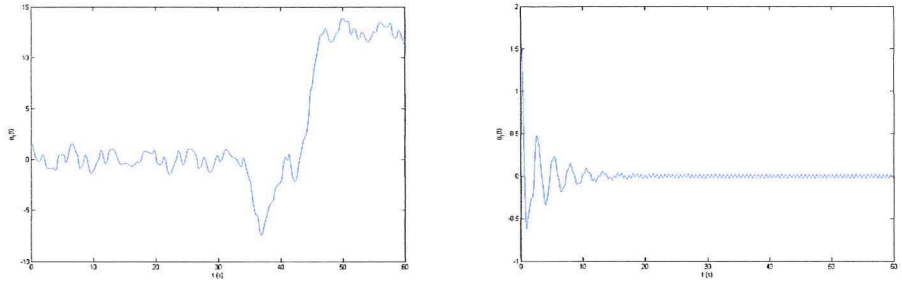

(c) $(10, 1)$ (d) $(10, 10)$

Figure 14: Various behaviours of the time series $\theta_1(t)$ for damped and forced double pendulum. Each plot is labelled with a vector (F, φ) indicating the amplitude of the external force and the frequency of forcing, with parameters $F_1 = F_2 = F$ and $\varphi_1 = \varphi_2 = \varphi$, i.e. the magnitude of the force and the frequency it is applied is the same for both the inner and outer pendulums. Damping constant is kept at $k = 1$. All figures have initial condition $\theta_1(0) = 90^o, \theta_2(0) = 0^o$ and no angular velocities when released.

but $t_1 - t_0 = \cdots = t_n - t_{n-1} = \Delta t$,

so summing up all λ_i and divide by n to get the average Lyapunov exponent λ, gives

$$\begin{aligned}\lambda &= \frac{\lambda_1 + \lambda_2 + \cdots + \lambda_n}{n} \\ &= \frac{1}{n}\left(\frac{1}{\Delta t}\ln\left(\frac{d(t_1)}{d_0}\right) + \frac{1}{\Delta t}\ln\left(\frac{d(t_2)}{d_0}\right) + \cdots + \frac{1}{\Delta t}\ln\left(\frac{d(t_n)}{d_0}\right)\right).\end{aligned}$$

Finally, if we let τ be the total interval of time evaluated over, then $n\Delta t = \tau$ so the average Lyapunov exponent is

$$\lambda = \frac{1}{\tau}\sum_{i=1}^{n}\ln\left(\frac{d(t_i)}{d_0}\right). \tag{17}$$

We can see from equation (17) that the units for λ is inverse time, or s^{-1}. Geometrically this derivation means we start with a reference trajectory and a comparison trajectory with close initial conditions, and follow them for a time interval Δt. Then when the growth deviates from exponential behaviour, we look for a new nearby path and start the process again; see figure 16. This iterative procedure to calculate the Lyapunov exponent can be programed in MATLAB. Good instructions for writing a program to calculate

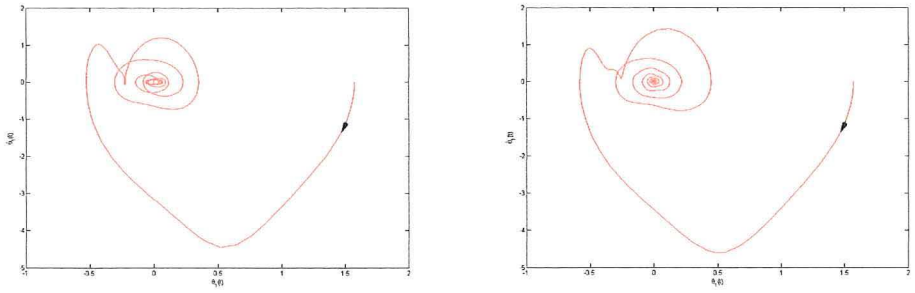

(a) $(1, 1)$ (b) $(1, 10)$

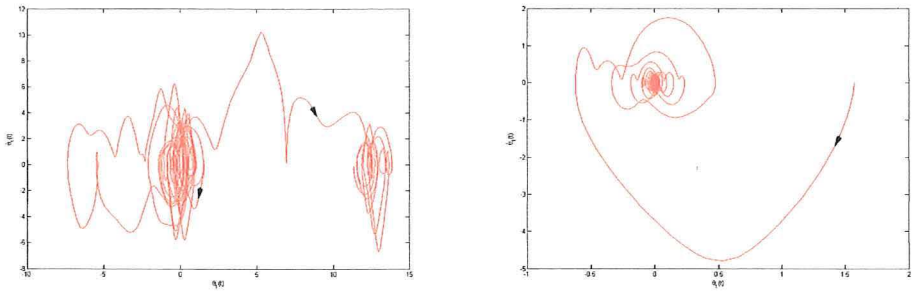

(c) $(10, 1)$ (d) $(10, 10)$

Figure 15: Various phase portraits corresponding to the same systems as in figure 14. Again, each plot is labelled with a vector (F, φ) indicating the amplitude of external force and the frequency of forcing; also with the parameters for damping and forcing set as $F_1 = F_2 = F$, $\varphi_1 = \varphi_2 = \varphi$ and damping constant $k = 1$. Arrows in the plots indicate the directions in phase space where the trajectories move with the passage of time. (a) and (d) shows when both forcing and its applied frequency have the same magnitude, elliptical limit cycles in phase space results. When external force is small but its applied frequency is high, as in (b), the trajectory converges to a point similar to a purely disspative system. The most interesting plot is (c) where the forcing amplitude is large but its applied frequency is low, giving behaviour different from the others. This is further explored in section 7 when strange attractors are discussed.

the exponent is given by Sprott [16]. Figure 17 shows the general situation where the calculated exponent value for a particular trajectory varies wildly at first but converges as more iterations are carried out.

There are a total of four Lyapunov exponents in the double pendulum system since it has a four dimensional phase space and there are as many exponents for a particular system as there are variables [10]. However, only the largest Lyapunov exponent is found by this method since the growth in the direction with the largest positive λ will have the most influence and will quickly swamp the increase in other directions. So the greatest Lyapunov exponent will dominate the exponential growth in the long run.

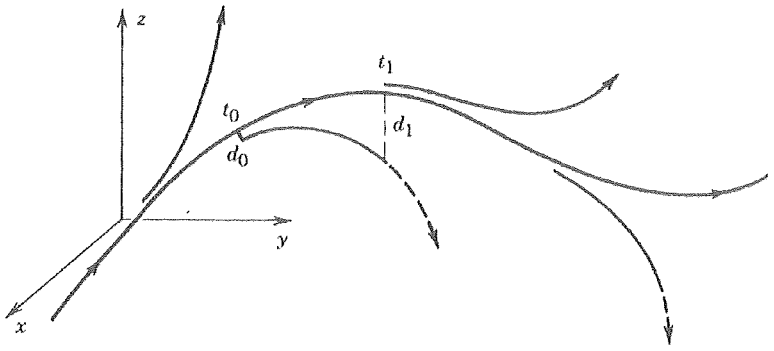

Figure 16: Illustration of the method to calculate the largest Lyapunov exponent; adapted from [11].

Three conditions exist for the Lyapunov exponent to indicate different behaviours:

- If $\lambda < 0$, then trajectories in phase space will converge together, signalling the system is dissipative.
- If $\lambda = 0$, distances between orbits will remain unchanged. An example of this is the conservative spring system performing simple harmonic motion where its paths in phase space trace out circular orbits which maintain a constant separation.
- If $\lambda > 0$, then orbits in phase space will diverge exponentially away from each other and so it is a prime indicator of chaos.

These statements can be justified by substituting the respective conditions into the definition of the Lyapunov exponent in equation (16).

The Lyapunov exponent for the double pendulum with large damping shown in figure 13 was found to be -0.2163 s^{-1}, as expected the λ value for that particular trajectory is negative. For the idealised system with a small release angle shown in figure 4, we find λ to be 0.0378 s^{-1}. Being very close to zero, it agrees well to the much more regular behaviour of small-angle-release. Again, for the idealised system with a large-angle-release in figure 5, we find λ equals 1.7421 s^{-1} so correctly indicating chaotic motion.

Figure 18 shows the numerical calculation of the Lyapunov exponent for initial condition $\theta_1(0)$ varying from 0° to 180°. We can see the general increase in λ as the release angle θ_1 also increases, meaning the larger the angle of release, the more sensitive to initial conditions the double pendulum becomes. Increasing the forcing amplitude F also results in overall larger Lyapunov exponents; as shown in figure 19. The critical value of F when λ goes from negative to positive indicates the point where forcing dominates over damping effects.

Note that although positive Lyapunov exponent is a necessary condition for chaos, it is not a sufficient one. In other words finding $\lambda > 0$ may not always be a definite indicator of chaos. It is possible to find exponential divergence of nearby trajectories even for systems that are not chaotic. A common situation where this phenomenon occurs is if the trajectories start off in the neighbourhood of a saddle point in phase space; for example when the pendulum is at its inverted position. The danger lies in assuming that the average Lyapunov exponent is positive based on only following the trajectories for a short time [7].

As emphasised by Shinbrot et al. [15], these behaviours are intrinsic to the chaotic nature of the double pendulum itself and are not due to imperfections or mechanisms of releasing the pendulum etc. Even if two exactly identical double pendulums were able to be constructed, we could not release them with the infinite precision necessary to disregard equation (16). *Any* differences however tiny is sufficient to give rise to the exponential growth in separations.

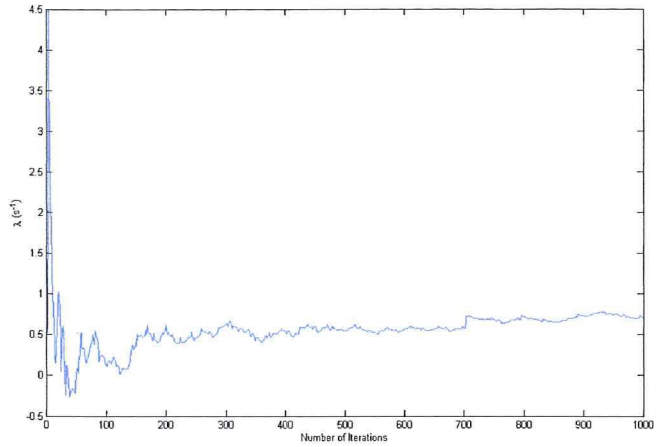

Figure 17: Numerical calculation of the Lyapunov exponent of a particular forced and damped double pendulum trajectory showing the intermediate exponent values at each iteration step. This graph gives the general situation where λ varies erratically at first but converge to a certain value as more iterations are performed. A suitable choice of the constant distance to restart the trajectories, d_0, is about one thousand times larger than machine precision [16], so $d_0 \approx 10^{-12}$.

7 Strange Attractors in the Double Pendulum

With damping and forcing introduced into the system in section 5, we can further explore the dynamics of the double pendulum. Here, we briefly investigate whether any strange attractors for the damped and forced double pendulum exist, and if so how does it behave.

A strange attractor is an attracting set in phase space on which chaotic orbits move [11]. The attractor consists of an infinite set of states that never repeat but are all contained in a finite volume of phase space. By varying the initial conditions and plotting the trajectories in the damped and forced double pendulum, we can see if the different paths will collapse onto a single trajectory. If this happens then it could indicate that a strange attractor is present; figure 20 shows this with trajectories clearly converging onto common paths. The multiple analogous paths seen in the plot is because the pendulum had rotated through by 2π and the trajectories is on the same attractor but shifted.

It is found that the optimal values for the damping and forcing parameters of the double pendulum is to keep the damping constant moderately high with a large amplitude force but relatively small forcing frequency, as evident by the results in figure 15. So the parameters are fixed with $k_1 = k_2 = 1$, $F_1 = F_2 = 10$ and $\omega_1 = \omega_2 = 1$.

Singling out a particular trajectory from figure 20 that lies on the attractor and plotting its orbit in phase space gives us a more geometric detail of this strange attractor. An arbitrary initial condition of $\theta_1(0) = 43^\circ, \theta_2(0) = 0^\circ$ and no initial angular velocity is chosen, some of its phase space orbits are shown in figure 21 with definite geometrical shapes visible. By using different colours to represent the distinct trajectories (figure 22), and more trajectories altogether (figure 23), we can view the behaviour of each path more clearly. A three dimensional view of the attractor in figure 24 shows that it is actually made up of many layers; needing an extra dimension to reveal it.

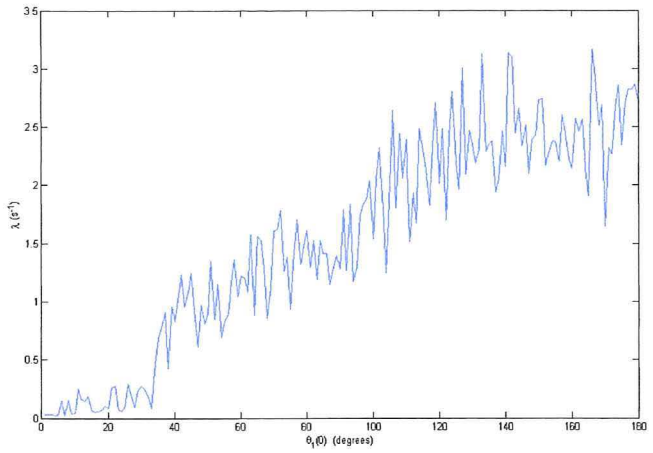

Figure 18: Lyapunov exponents for the undamped and unforced double pendulum with initial condition $\theta_1(0)$ varying from 0^o to 180^o at increments of 1^o at a time. With $\theta_2(0) = \dot{\theta_1}(0) = \dot{\theta_2}(0) = 0$. We can see that λ increases with the release angle, thus showing large-angle-releases are more sensitive to change.

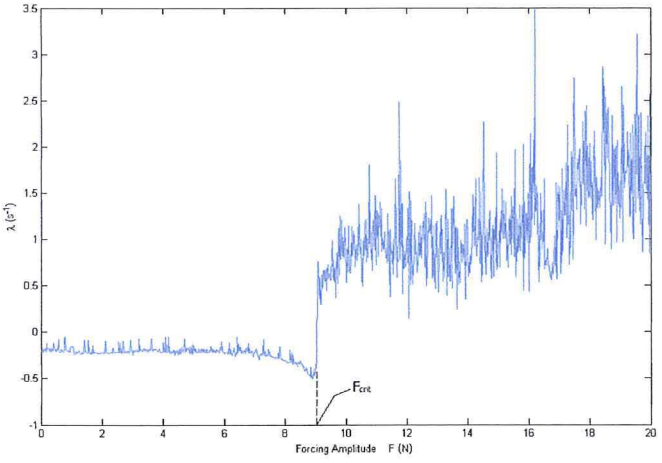

Figure 19: Lyapunov exponents for a varying forcing amplitude F. Initial release angle is kept at $\theta_1(0) = 115^o$ and $\theta_2(0) = 0^o$ with no initial angular velocities. λ is negative for small amplitudes of forcing but suddenly jumps to a positive value at F_{crit}, meaning the system's paths has changed from converging together to diverging apart. For this particular initial condition, $F_{\text{crit}} \approx 9.04$ Newtons.

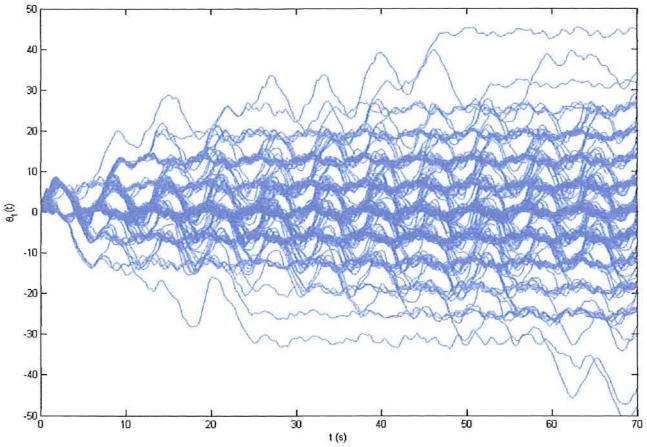

Figure 20: Various trajectories for $\theta_1(t)$ on the same plot with initial condition $\theta_1(0)$ ranging from 0 to π in increments of 0.01 radians, so 314 trajectories plotted altogether. All initial conditions for other variables kept at zero. Numerous trajectories have converged into single paths indicating a strange attractor.

8 Conclusion

It is astonishing that such a simple mechanical device can exhibit these rich and complicated behaviours. The double pendulum equations of motion derived produced a pair of highly nonlinear coupled differential equations of the second order which hinted at its complexity. Using these equations we have successfully carried out various investigations demonstrating the chaotic nature of the double pendulum.

Time series plot show irregular trajectories that model the chaotic motion of a real double pendulum. Intriguing patterns emerge as time-for-first-flip is plotted against initial conditions of the release angle $\theta_1(0)$ and $\theta_2(0)$. Furthermore, there does not seem to be any reasons for the pendulum not to flip in regions of the plot satisfying the energy constraints, but nevertheless these regions do appear and form swirling patterns that seem to resemble fluid flow. This may suggest that fluid mechanics can be used to analyse these plots.

Positive Lyapunov exponents calculated for different situations such as: large-angle-release, increased forcing amplitude and paths on the strange attractor, meant close trajectories will diverge exponentially from each other in agreement with the observations of sensitivity to initial conditions.

These results showed that even though there are a set of definite equations governing this system, it is still intrinsically unpredictable in the long run due to inevitable errors introduced either physically or numerically.

There are still many things to be investigated about the double pendulum; one of which is to see if changing the basic parameters of the system will have any significant effects on its behaviour, since throughout all investigations the unity parameter in equation (9) have been used. Another aspect to further explore might be to plot the 2nd or 3rd or nth time to flip and see what different patterns will emerge. Also, an investigation into how the value for F_{crit} that separate the effects of damping and forcing as measured by the Lyapunov exponent might change as initial conditions are varied could be worth while. With different forcing and damping combinations, other strange attractors may be able to be found.

The double pendulum provides a simple and yet dramatic demonstration of chaotic dynamics. The simplicity of the device generating wild and unexpected behaviour will if nothing, mesmerise the audience and leave them with a deep impression of chaos.

References

[1] Scienceworld - double pendulum. http://scienceworld.wolfram.com/physics/DoublePendulum.html. Retrieved 17 Dec 2007.

[2] D. Acheson. *From Calculus to Chaos - An Introduction to Dynamics.* Oxford University Press, New York, 1998.

[3] G. L. Baker and J. P. Gollub. *Chaotic Dynamics - An Introduction.* Cambridge University Press, Cambridge, 1990.

[4] M. Beilby, G. Gonzalez, M. Duffy, A. Stuver, and J. Poker. Development of a double pendulum for gravitational wave detectors. *ArXiv.org/gr-qc/9911027*, November 1999.

[5] P. Collet and J. Eckmann. *Concepts and Results in Chaotic Dynamics: A Short Course.* Springer-Verlag, Berlin, Heidelberg, 2006. pp. 116-122.

[6] J. Gleick. *Chaos: Making a New Science.* Viking Penguin Inc., New York, NY, U.S.A., 1987. pp. 230.

[7] R. Hilborn. *Chaos and Nonlinear Dynamics: An Introduction for Scientists and Engineers.* Oxford University Press, New York, 1994. pp. 176.

[8] T. Kibble and F. Berkshire. *Classical Mechanics.* Addison Wesley Longman, Edinburgh Gate, Harlow, Essex, England, 4th edition, 1996.

[9] R. Levien and S. Tan. Double pendulum: An experiment in chaos. *Am. J. Phys.*, 61(11):1038, November 1993.

[10] J. Marion and S. Thornton. *Classical Dynamics of Particles and Systems.* Harcourt College Publishers, 4th edition, 1995. pp. 138.

[11] F. C. Moon. *Chaotic and Fractal Dynamics - An Introduction for Applied Scientists and Engineers.* John Wiley and Sons, Inc., New York, NY, U.S.A., 1992. pp. 382.

[12] F. C. Moon. *Applied Dynamics with Applications to Multibody and Mechatronic Systems.* John Wiley and Sons, Inc., New York, NY, U.S.A., 1998.

[13] P. Nahin. *When Least is Best.* Princeton University Press, Princeton, New Jersey, 2004. pp. 231-238.

[14] R. Penner. The physics of golf. *Reports on Progress in Physics*, 66:131, 2003.

[15] T. Shinbrot, C. Grebogi, J. Wisdom, and J. Yorke. Chaos in a double pendulum. *Am. J. Phys.*, 60(6):491, June 1992.

[16] J. C. Sprott. Numerical calculation of largest lyapunov exponent. Retrieved 24 Jan 2008. http://sprott.physics.wisc.edu/chaos/lyapexp.htm.

[17] J. Torok. *Analytical Mechanics with an Introduction to Dynamical Systems.* John Wiley and Sons, Inc., New York, NY, U.S.A., 2000. pp. 88-93.

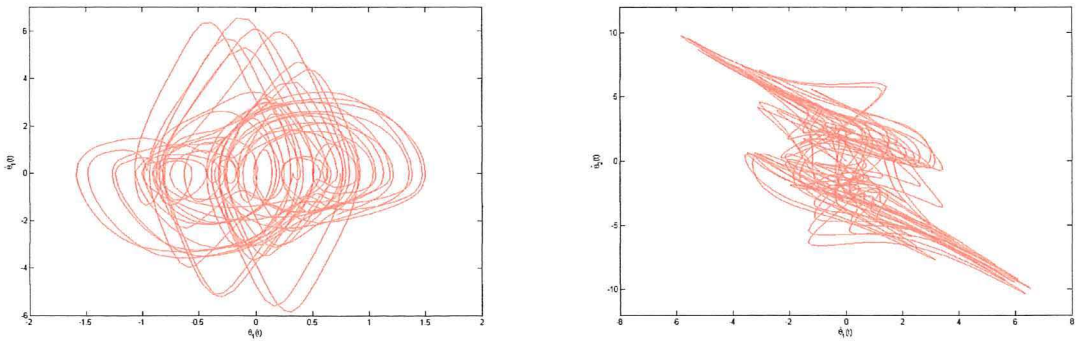

(a) (b)

Figure 21: Phase portraits of a strange attractor evaluated to 70 seconds on a damped and forced double pendulum system. (a) shows the phase space behaviour of θ_1 against $\dot{\theta_1}$, (b) the phase space behaviour of $\dot{\theta_1}$ against $\dot{\theta_2}$. Definite shapes can be seen suggesting there is some order amongst the chaos. Lyapunov exponent calculation for this trajectory gives $\lambda = 0.6845$.

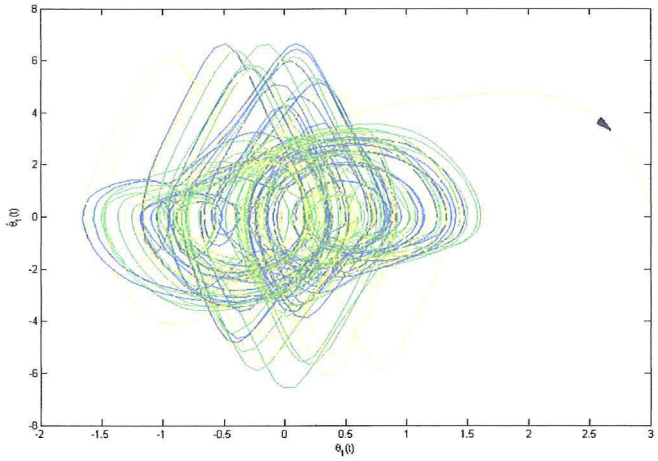

Figure 22: Phase space plot of three trajectories with slightly different initial conditions for $\theta_1(0)$, showing paths converging onto the attractor. The arrow on the yellow path indicates the direction of its motion in phase space. That particular trajectory is about to shift by 2π and trace out the same but shifted attractor. Only three colours were used because too many colours resulted in an indistinguishable blur.

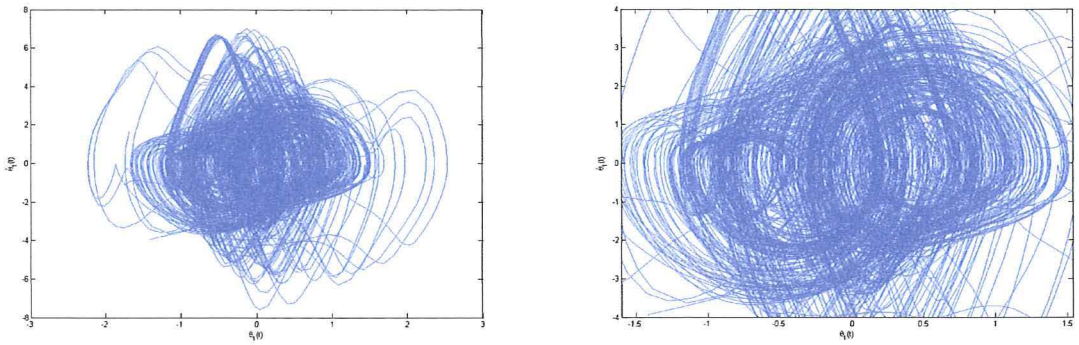

(a) (b)

Figure 23: Multiple trajectories plotted in phase space with initial conditions ranging from 0 to 0.2 radians incremented by 0.01 at a time. (a) shows the strange attractor in the phase plane of θ_1 against $\dot{\theta}_1$ with the total time evaluated being 60 seconds, (b) gives a zoomed in view of the attractor. Only paths that stay between $-\pi$ and π are plotted.

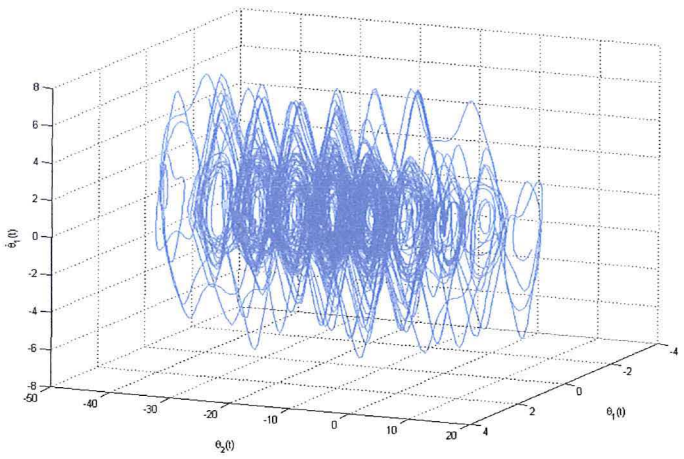

Figure 24: 3D view of the strange attractor shown in figure 23.